DYNAMIC ESTIMATION OF BANK-PROPELLER INTERACTION EFFECT ON SHIP MANEUVERING USING CFD METHOD COUPLED TO 6DOF ALGORITHM

S. KAIDI[†*], H. SMAOUI[†*], P. SERGENT[†] and A. OUAHSINE[*]

[†] CEREMA-DtecEMF, 60280 Margny-lès-Compiègne, France
e-mail: sami.kaidi@cerema.fr - Web page: http://www.cerema.fr

[*] Sorbonne universités, Université de technologie de Compiègne, laboratoire Roberval,
60203 Compiègne cedex, France
e-mail: sami.kaidi@utc.fr - Web page: http://www.utc.fr

Key words: CFD simulation, Bank-propeller interaction, Dynamic estimation, 6DOF, Dynamic mesh, User-defined function

Abstract. This paper presents a numerical investigation of ship maneuvering under the combined effect of the bank and propeller. The incompressible turbulent flow with free surface around the self-propelled hull form is simulated using a commercial CFD software (Fluent). In order to estimate the dynamic effect of bank and propeller, the CFD model with the dynamic mesh setting is coupled to the 6DOF module to compute the ship motion due to hydrodynamic forces. The numerical simulations are carried using the equivalent experiment conditions. The validation of the CFD model is performed by comparing the numerical results to the experimental data.

1 INTRODUCTION

The transport by inland waterways is considered as a complementary means to rail and road transport. These last year's this mode of transport has seen a significant traffic increase due to the encouragement of the various states to the exploitation of waterways, on the one hand to relieve the other modes of transport and on the other hand for its ecological quality.

This navigation environment presents a major risk which concerns mainly the accidents due to the ships controllability. Contrary to the maritime navigation, the waterways navigation environment plays an important role on the ship maneuverability (channel geometry, water depth, bank distance, ...)

In the present work, we focus on the study of banks effect. Norrbin [1], is at the origin of the first works on the interaction Ship-bank. The conclusion of its experimental works has shown a significant impact of the banks on the trajectory of the ships. This study is improved later by taking into account new parameters; bank slope, hull form, water depth, bank height and ship

speed [2,3]. An empirical and mathematical formula [4] are proposed to estimate the bank-ship sway force and yaw moment for ship handling simulator.

With the fast development of the computer technology and the commercial CFD software. The CFD method has interested the inland community. This method is used mostly and it proved its ability to predict the ship maneuvering hydrodynamic forces (lateral force and yaw moment) [5].

In this paper, a dynamic study is proposed to predict the combined effect bank-propeller on the ship maneuverability. CFD model coupled to Six degrees of freedom module is used to estimate the different hydrodynamic forces acting on hull and to simulate the motion behavior of the ship by varying the ship speed and ship position to bank. From Six degrees of freedom, three are allowed; two translations along the x and y-axis and one rotation along the z-axis. The other three freedom (draft, roll and pitch) are set. The dynamic mesh is adopted in order to correct the deformed mesh around the ship during its movement.

The first section of results concerns the validation of the numerical model with measurements tests conducted in ULG (Liege University) towing tank, several configurations are compared. The second section shows the different simulations performed to study the ship behavior under the bank-propeller effect. The last section of results provides a general analysis and discussion about the influence of the combined effect bank-propeller compared to the simple effect of bank on the ship maneuverability.

2 PROBLEM FORMULATION

2.1 Governing equations

The governing equations for mass and momentum conservation are the Reynolds Averaged Navier-Stokes (RANS) equations for incompressible flow, given by:

$$\frac{\partial \rho}{\partial t} + \frac{\partial (\rho u_i)}{\partial x_i} = 0 \qquad (i = 1,2,3) \qquad (1)$$

$$\frac{\partial (\rho u_i)}{\partial t} + \frac{\partial (\rho u_i u_j)}{\partial x_j} = \frac{\partial}{\partial x_j}\left[\mu\left(\frac{\partial u_i}{\partial x_j} + \frac{\partial u_j}{\partial x_i} - \frac{2}{3}\delta_{ij}\frac{\partial u_i}{\partial x_i}\right)\right] - \frac{\partial P}{\partial x_j} + \frac{\partial (\rho \overline{\acute{u}_i \acute{u}_j})}{\partial x_j} \qquad (i = 1,2,3) \qquad (2)$$

$$\rho = \sum_{n=1}^{2} \alpha_n \rho_n \ , \qquad \mu = \sum_{n=1}^{2} \alpha_n \mu_n \qquad (3)$$

here $x_{i(j)} (i = 1,2,3)$ are Cartesian coordinates; ρ is the water density and t is time; $u_{i(j)} (i = 1,2,3)$, P and μ are velocity components, pressure and dynamic viscosity respectively; α is the phase fraction, $n = 1,2$ denotes the fluid phase number (water and air); δ_{ij} is the Kronecker delta; $\acute{u}_{i(j)}$ represents the fluctuating velocity; $-\rho \overline{\acute{u}_i \acute{u}_j}$ denote the Reynolds stresses;

$$-\rho\overline{\acute{u}_i\acute{u}_j} = \mu\left(\frac{\partial u_i}{\partial x_j}+\frac{\partial u_j}{\partial x_i}\right)-\frac{2}{3}\left(\rho k+\mu_{ij}\frac{\partial u_i}{\partial x_i}\right)\delta_{ij} \qquad (i=1,2,3) \qquad (4)$$

The Reynolds stresses introduce a new variables, which makes the equation system (Equations 1 and 2) not closed. To close and solve this system, several complementary mathematical models with additional equations are proposed. This models are called, turbulence models. In the present paper, the implicit Menter Shear Stress Transport (SST) $k-\omega$ model is adopted.

2.2 CFD solver

In this work, the incompressible free surface flow around the ship hull is studied using the commercial RANS code "Ansys-Fluent" based on the finite volume method. The pseudo transient Pressure-Based Coupled Algorithm is adopted to compute the pressure-velocity coupling; the (PRESTO) interpolation method is selected to compute the cell-face pressure.

To capture the free surface in air-water interface, the Volume Of Fluid (VOF) method is employed. Using this method, the numerical grid is fixed in space, and the prediction of free surface deformation is determined by solving an additional transport equation.

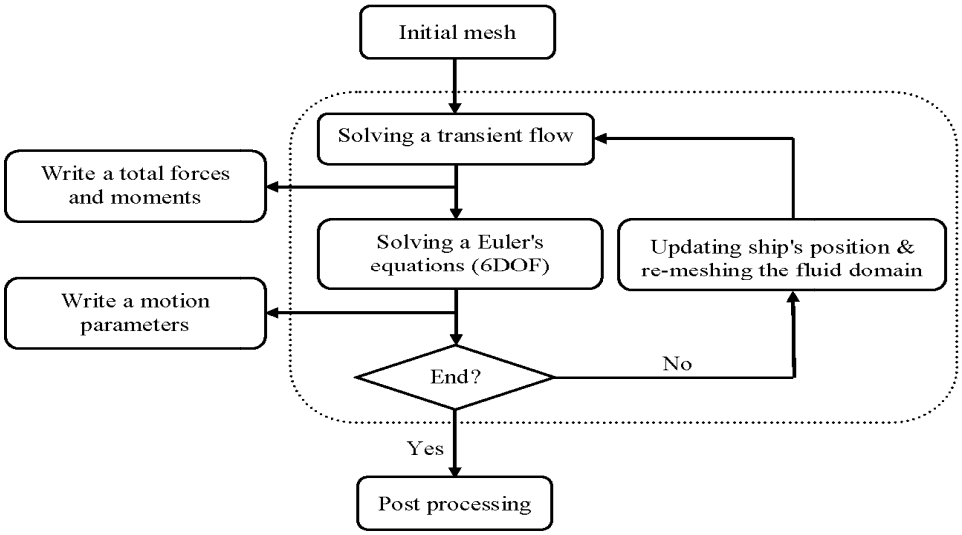

Figure 1: Flowchart of CFD model operation

2.3 Ship hull

The self-propelled (135x11,40m) is one of the most container-ship used in waterways transport. In this investigation, the hull form of this ship is selected for both test cases, experimental and CFD. No rudder and no propeller are included for the validation tests. The propeller will be included only in the last section of this work. The ship hull geometry for tested model is presented at scale of 1/25. Table 1 and Figures 2 and 3 show the main characteristics and the body lines of the hull form.

Table 1: Geometric parameters of ship hull

	Length (L)	Beam (B)	Draft (T)	Block coefficient (C_B)	Wetted surface (WS)	Cross area of ship (CS)
Real model	135 m	11.4 m	2.5 m	0.899	2104.8 m²	34.114 m²
Scaled model (1/25)	5.4 m	0.456 m	0.1 m	0.899	3.367 m²	0.0545 m²

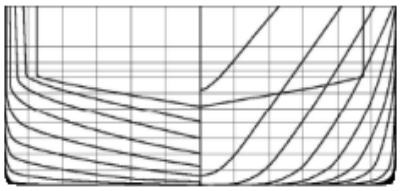

Figure 2: Lines plan of the self-propelled ship

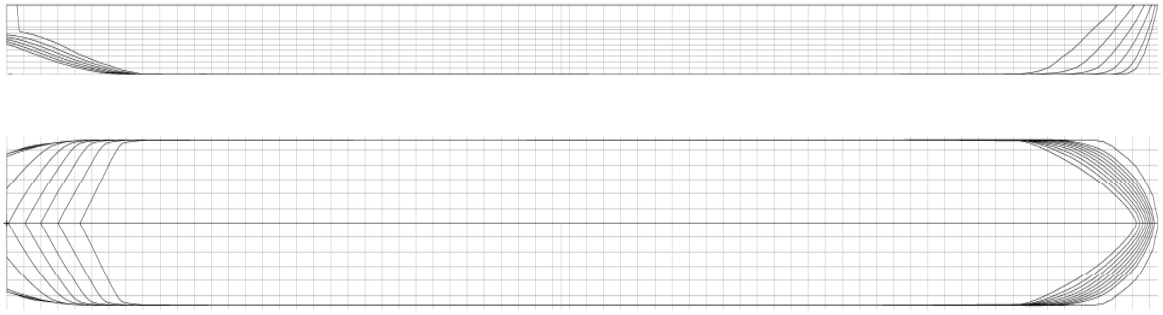

Figure 3: Lines plan of the self-propelled ship

3 PRESENTATION OF THE EXPERIMENTAL TESTS

The tests conducted for this work are realized in the towing tank at the Liege University, Figure 4-a and 5. Table 2 shows the geometrical characteristics for the five tested configurations (three channel widths and three under keel clearance). The test device consists of a towing carriage that tow the ship model with a speed which can reach 5 m/s and a balance to measure the forces and moments acting on the ship model.

Table 2 : Scaled channel dimensions

Test type	Length (L)	Top width (B)	Bottom width (b)	Bank slope (α)	UKC (T)
Water depth (h) 0.18 m	50 m	2.15 m	0.72 / 1.44 / 2.88 m	27°	0.1 m
Water depth (h) 0.2 m	50 m	2.22 m	1.44 m	27°	0.1 m
Water depth (h) 0.24 m	50 m	2.38 m	1.44 m	27°	0.1 m

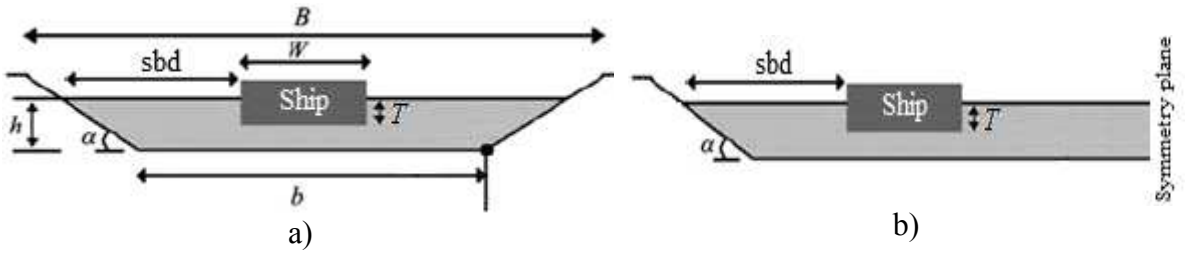

Figure 4: Channel geometry; a) two banks, b) one bank

Figure 5: Illustration of the test tank

4 VALIDATION OF NUMERICAL MODEL

To validate the CFD model, the numerical results of ship resistance are compared to the measurements carried in towing tank. Five geometrical configurations are simulated, Three water depths and three bottom widths. For each configuration, different ship speeds varying between 0.222 and 0.575 m/s (between 4 and 10 km/h in real scale) are tested. Due to the study domain symmetry for the centered ship cases, only the half of the domain is considered and meshed. For the other cases, the whole domain is meshed.

4.1 Boundary conditions

The following figure show the standard computational domain with different boundary conditions. The boundary conditions shown in figure 6 are detailed in Table 3.

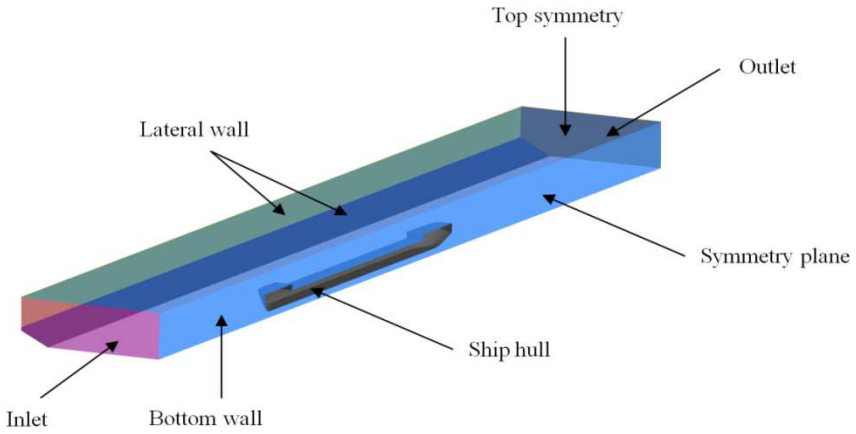

Figure 6: Applied boundary conditions

Table 3 : Boundary conditions

Inlet	Pressure inlet	Free surface level and Normal velocity
Outlet	Pressure Outlet	Specified Free Surface Level
Ship hull	wall	No Slip & Wall Roughness (Default)
Lateral wall & Bottom wall	Moving wall	No Slip & Motion: x- velocity
Symmetry plane & Top	Symmetry	Default

4.2 Grid settings

For the validation cases, the study domain is meshed with a mixed mesh. The region around the ship hull is meshed using ~467678 non-structured tetrahedral elements, and the rest of the study region is meshed with ~313600 structured hexahedral elements.

To resolve the flow more precisely, the mesh is appropriately refined at the free surface for a better capturing and near the ship to estimate the hydrodynamic forces (pressure and viscous forces) acting on the hull form more exactly (Figure 7). This mesh quality is chosen after a mesh convergence study. For the dynamic simulations, the dynamic mesh is used. The parameters that control the mesh quality are set such that the mesh remains refined around the ship throughout the simulation.

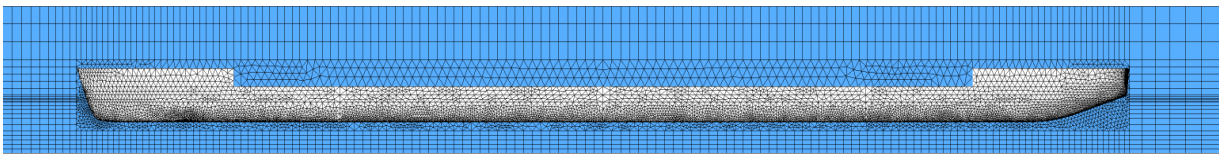

Figure 7: Mesh distribution

4.3 Centered ship results

The figure 08 shows the comparison between the computed and measured ship resistance. By analyzing these graphs, we note that the both results are similar and have the same allure.

We observe also, that for all tests, the relative error depends on two parameters, the ship speed and the confinement of navigation environment. Where, the error increase by increasing ship speed and by reducing the wetted section of the channel. In some cases the error can reach 18%.

The difference cited above, can be explained by the use of some simplifying assumptions. Among the assumptions that can influence the numerical results is the negligence of the ship squat. For a high speed in a restricted channel, the ship sinks significantly in water and

usually causes an additional resistance. Hence, ignoring the modeling of this phenomenon, it generates a pronounced difference between the two results.

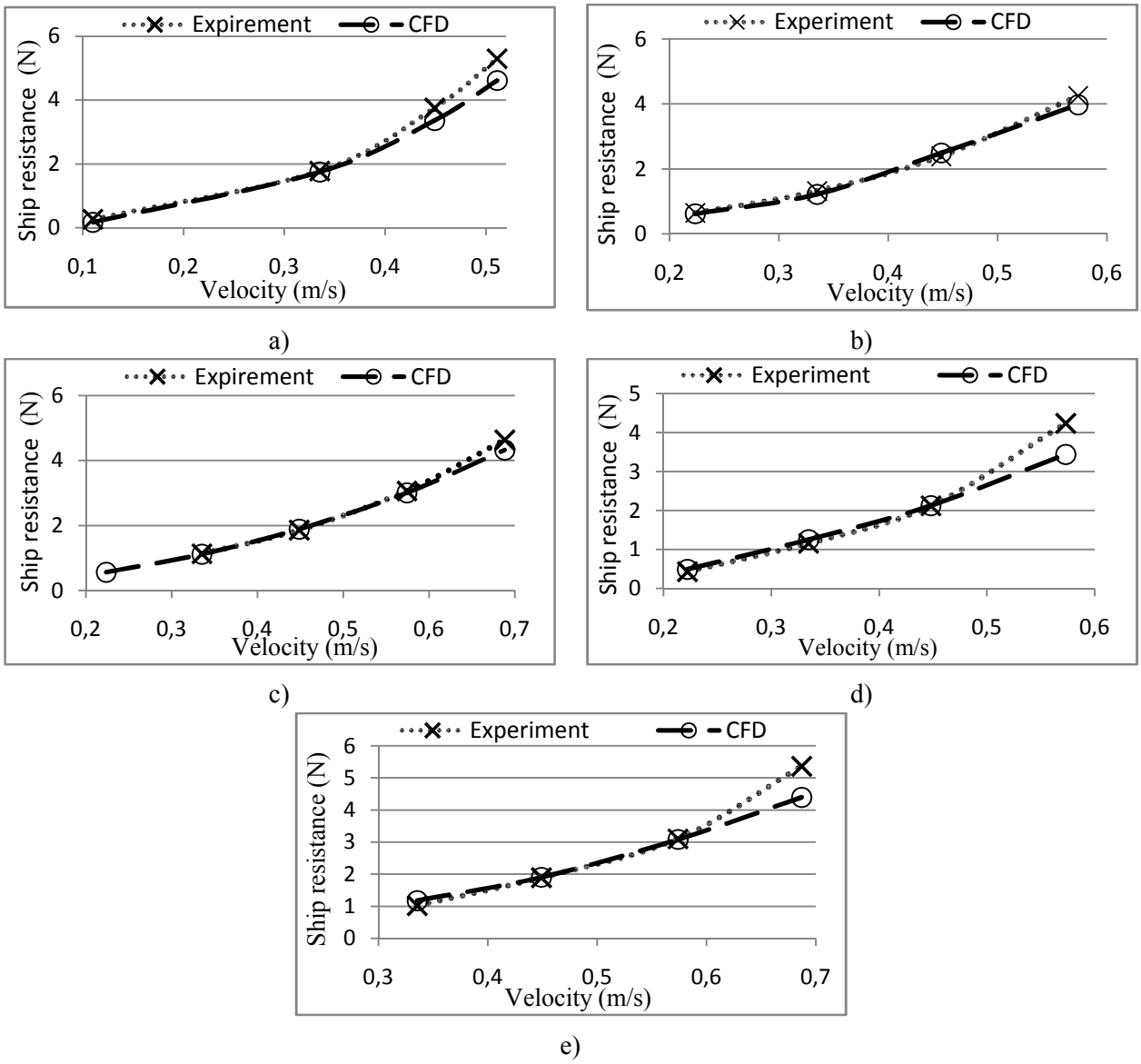

Figure 8: Comparison of the CFD results to measurements; a) h=0.18 m & b=0.72 m, b) h=0.18 m & b=1.44 m, c) h=0.18 m & b=2.88 m, d) h=0.2 m & b=1.44 m, e) h=0.24 m & b=1.44 m

4.4 Offset ship position results

In this section, an additional validation tests are performed. Two offset positions of the ship to the bank (0.445 m and 0.228 m, see figure 4) are tested for four different speeds. Figure 9 present the comparison between the computed and experimental results. An identical allure of the computed and measured results is observed. This figure shows also that the ship resistance is well estimated by the CFD model for the both ship positions when the ship speed is less than 0.45m/s. However, for important ship speed (0.575 m/s), we note a significant error

especially when the ship is closer to the bank. This difference is related to the pressure variation along the ship hull caused on one hand to the important water level variation on the bank side and in the other hand to the ship squat.

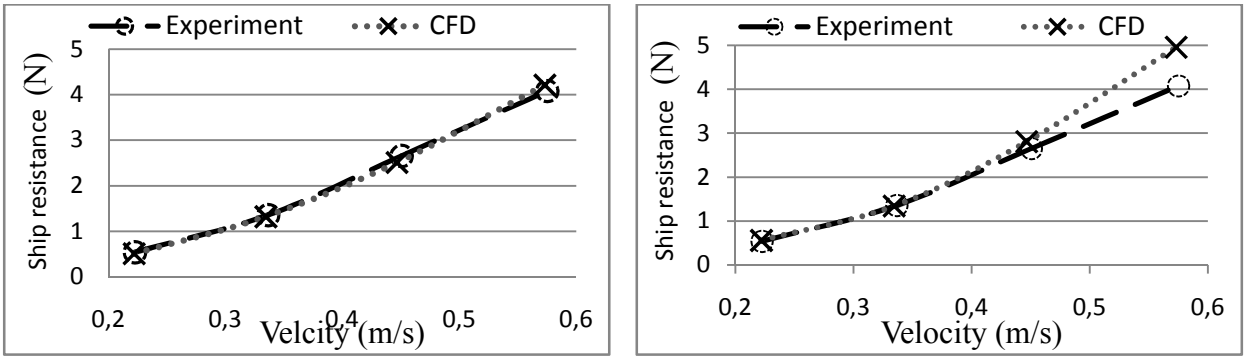

Figure 9: Ship resistance comparison for ship position 0.445 m left and 0.228 m right

5 TESTS RESULTS

The validated numerical model is used in order to perform a comparative study about the dynamic effect of the bank on the ship maneuverability. This section is devised into two parts: the first part concerns the influence of the ship-bank distance (*sbd*) and the ship speed, and the second part treat the influence of the propeller system. For the next simulations, to estimate the force associated to the bank, we consider only one bank and the other bank it is assumed far and can be modeled by a symmetry plane condition.

5.1 Influence of ship-bank distance

In this first part of results, we study the dynamic effect of the bank by varying the ship-bank distance. The table 4 illustrate the four simulated configurations. For these simulations we use an average ship speed of 8km/h that correspond to 0.45m/s in the scaled model. Figure 10, shows the ship speed profile. It is assumed that the initial ship speed is zero and it increases linearly to reach 0.45m/s in 0.5 second. This assumption is used to overcome the side effects related to the waves abruptly generated when the initial ship speed different to zero and that can affect the ship trajectory.

Table 4 : Channel dimensions

Test type	Bank-Ship distance (sbd)	Bank slope (α)	Channel cross area (C_C)	Water depth (h)
Simulation cases	0.2 / 0.4 / 0.6/ 0.8m	90°	8.07 m²	0.18 m

The geometry of the computational domain is presented in figure 4-b. The adoption of the user defined function (UDF) is essential to simulate a constant ship speed.

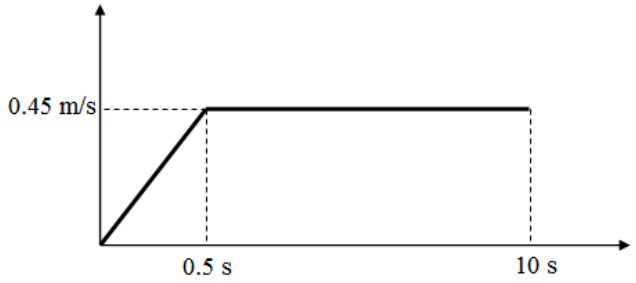

Figure 10: Ship speed profile

The figures 11 and 12 present respectively the time-based variation of yaw angle and lateral motion of the ship as function of the ship-bank distance. The obtained results show clearly the influence of this parameter on the behavior of the ship motion. The results indicate that the ship is more affected when the distance between the ship and the bank is decreased. From these figures we note that the ship starts to deviate early when it is close to the bank and the yaw angle can reach 5° in 10 second.

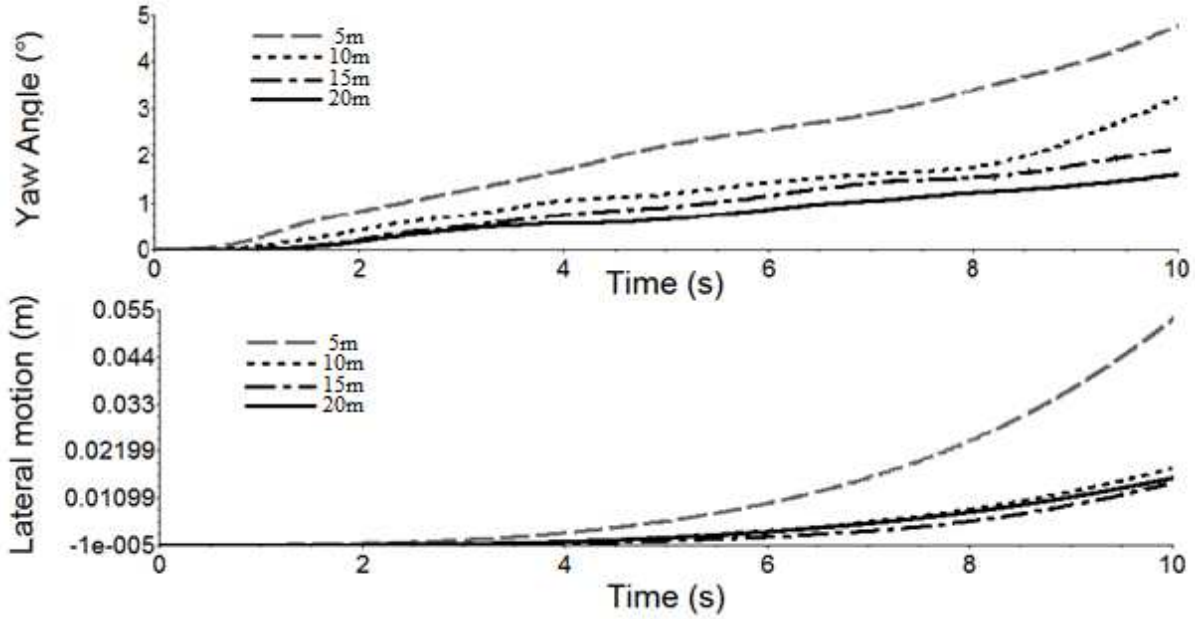

Figure 11: Temporal evolution of yaw angle and lateral motion of the ship as function of the distance to bank

By analyzing the figure 11, it is observed that the temporal evolution of the yaw angle is not completely linear. The yaw angle present some variation which can be due to the ship inertia. This variation can be seen clearly in the case of the lower ship-bank distance.

The temporal variation of the non dimensional sway force and yaw moment are presented in the figure 12. The general appearance show that the both forces depend strongly to the ship-bank distance. Unlike a classical studies that consider a fixed ship, when the ship is moving the non-dimensional sway force and yaw moment are not constant and their behavior is completely non-linear (periodic). We note also that the forces remain lower in the simulation beginning until 3 second, otherwise, the forces increase proportionally to the ship-bank distance reduction.

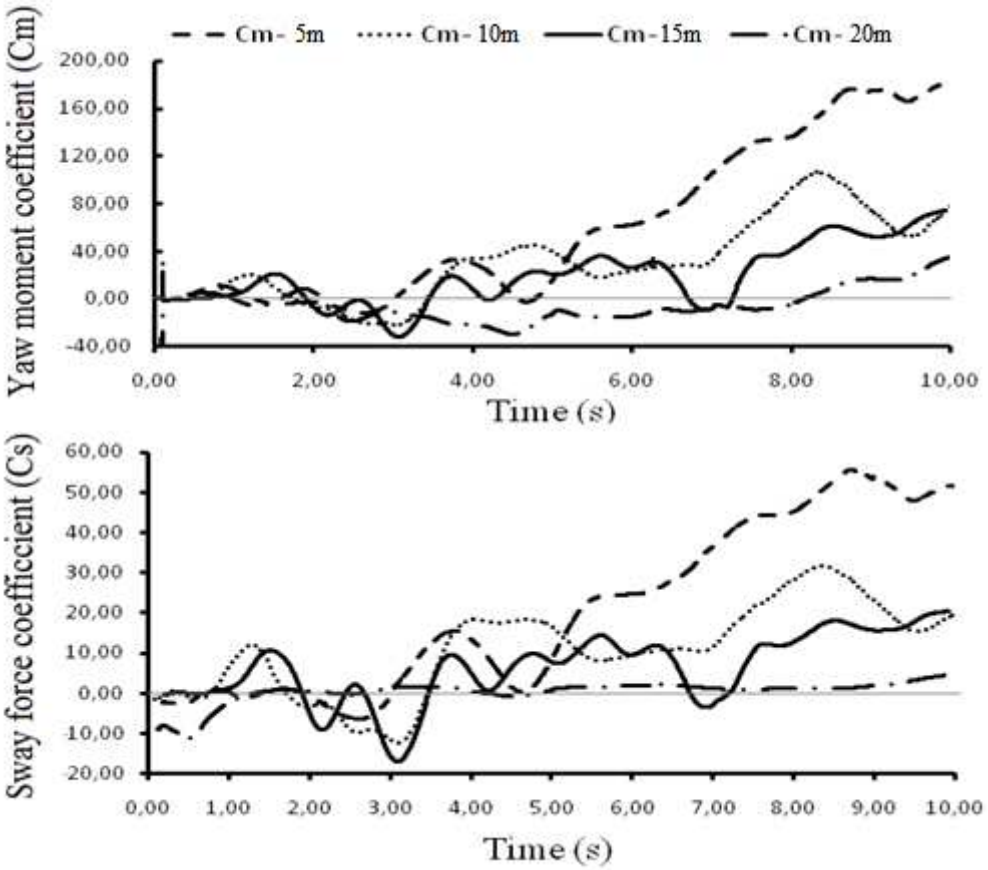

Figure 12: Temporal evolution of yaw moment and sway force coefficients as function of the distance to bank

5.2 Influence of ship speed

In this section we investigate the influence of the ship speed parameter. To carry this investigation, we take a lowest lateral distance *sbd*=0.2 (5m in real model). The simulation results of the ship yaw angle and the lateral displacement as function of the ship speed are presented in figure 13. From this figure it can be seen that the bank effect is important for a high ship speed. The yaw angle can reach 8°, and the lateral displacement of the ship can reach 0.2m in scaled model that correspond to 5m in real scale. For a lower speed (less than 0.3m/s) the ship motion is not greatly affected. By analyzing yaw angle variation, we observe three phase, the first is between 0 and 1.8 second, the second is between 1.8 and 4.8 second and the last phase is from 4.8 second to the simulation end. In each phase, it can be seen that the ship accelerates and then decelerates. This effect is related to the variation of the resultant moment generated by the different forces acting on the ship including the inertia force.

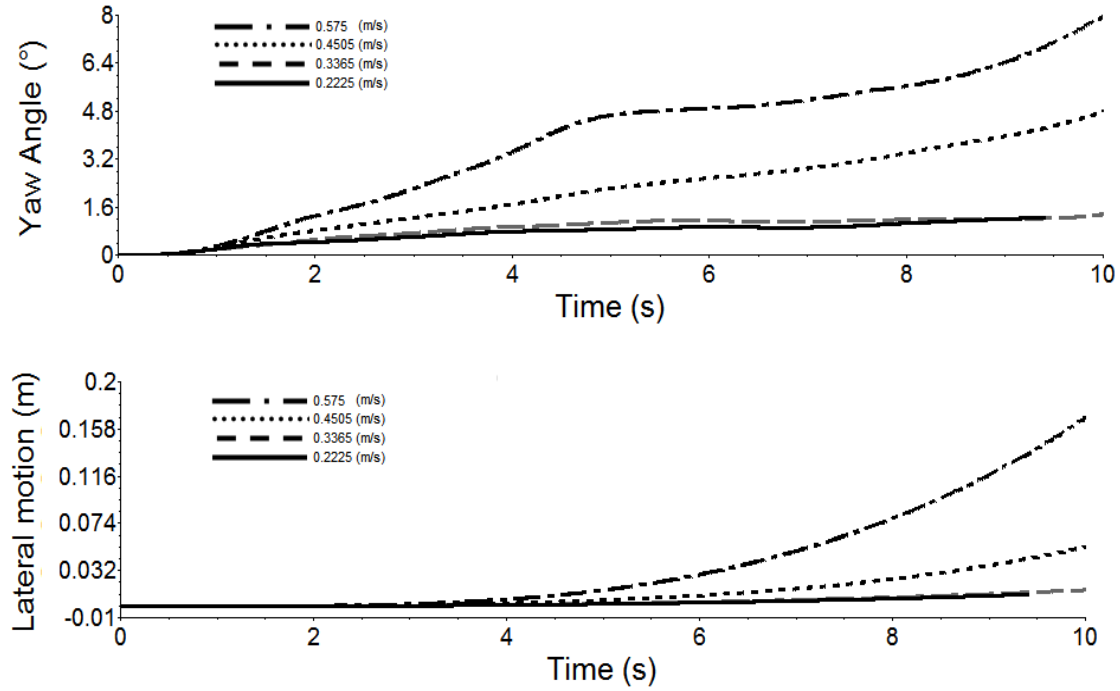

Figure 13: Temporal evolution of yaw angle and lateral motion of the ship as function of the ship speed

5.3 Influence of propeller (Results of this part will be available soon, 15/06/20115)*

In this part, the numerical model is modified by including the propeller. The first results present the preliminary study of the current line around the ship with and without the propeller. The second results concern the dynamic study of the combined effect propeller-bank on the ship maneuvering.

The propeller effect is modeled by adding an additional body force F_P in equation 2 [6]. This total force can be expressed by three components: the axial force F_{PX} , the tangential force F_{PT} and the radial force F_{PR}. In the present work, the radial force is considered zero. The other forces are normalized to the simulations scale. These forces are written as below:

$$F_{PX} = A_x r^* \sqrt{1 - r^*} \tag{5}$$

$$F_{P\theta} = A_\theta \frac{r^* \sqrt{1 - r^*}}{r^*(1 - r_h') + r_h'} \tag{6}$$

$$F_{Pr} = 0 \tag{7}$$

Where $r^* = (r' - r_h')/(1 - r_h')$; $r' = r/R_P$ and $r_h' = R_H/R_P$. r is the actuator disc radius, R_P=..., the propeller radius and R_H =.. is the hub radius, and A_x and A_θ are constants given by:

$$A_x = \frac{105}{8} \frac{T_P}{2\pi\Delta(R_P - R_h)(3R_h - 4R_P)} \tag{8}$$

$$A_\theta = \frac{105}{8} \frac{Q_P}{2\pi\Delta R_P(R_P - R_h)(3R_h - 4R_P)} \tag{9}$$

with

$$T_P = \frac{C_T}{2}\pi\rho V_b^2 R_P^2 \tag{10}$$

$$Q_P = K_Q \rho n^2 (2R_P)^5 \tag{11}$$

T_P and Q_P are the normalized total thrust and torque of propulsion system. C_T and K_Q are the thrust and torque coefficients; n is the number of rotations per second (rps) and Δ is the actuator disc thickness.

6 CONCLUSIONS

Dynamic analysis of the bank effect is performed using a CFD model coupled to the 6DOF algorithm. The main results obtained by this numerical model are:

- The release of the lateral degree of freedom help to recurrence the real bank effect
- The dynamic analysis of the bank effect is important because it consider the ship inertia and shows the temporal evolution of the different forces acting on the ship
- The bank effect depends strongly to the ship-bank distance and to the ship speed
- The bank effect depends also to the additional force caused by the propeller.

REFERENCES

[1] Norbin, N. *Bank effects on a ship moving through a short dredged channel*, 10th Symposium on naval hydrodynamics, combridge, MA, USA, (1974)

[2] Ch'ng, PW. Doctors, LJ. and Renilson, MR. *A method of calculating the ship-bank interaction forces and moments in restricted water*. Int Shipbuild Prog, 40(421), (1993)

[3] Duffy, J. T. *The effect of the channel geometry on ship operation in a port*. 30th PIANC-AIPCN congress, Sydney, (2002).

[4] Lataire, E. Vantorre, M. Laforce, E. Eloot, K. Delefortrie, G. *Navigation in confined water: influence of bank characteristics on ship-bank interaction*. The maneuvering Committee, Final Report and Recommendations to the 24th ITTC, (2005)

[5] Lo, DC. Su, DT. Chen, JM. *application of computational fluid dynamics simulations to the analysis of bank effects in restricted waters*. J Navig, 62, pp. 477-491, (2009).

[6] Sheng Cheng, JI. Ouahsine, A. Smaoui, H. Sergent, P. (2014). *3D Numerical modeling of Sediment resuspension induced by the compounding effects of ship-generated waves and the ship propeller*, Journal of Engineering Mechanics(ASCE) Volume 140, Issue 6 (June 2014)